Proc. Natl. Acad. Sci. USA
Vol. 86, pp. 1138–1142, February 1989
Biochemistry

Growth-rate-dependent regulation of 6-phosphogluconate dehydrogenase level mediated by an anti-Shine–Dalgarno sequence located within the *Escherichia coli gnd* structural gene

(translation control/antisense RNA/gene regulation)

PENELOPE CARTER-MUENCHAU AND RICHARD E. WOLF, JR.*

Department of Biological Sciences, University of Maryland Baltimore County, Baltimore, MD 21228

Communicated by Hamilton O. Smith, November 1, 1988 (received for review August 15, 1988)

ABSTRACT **Previous work has shown that in *Escherichia coli* K-12 growth-rate-dependent regulation of expression of 6-phosphogluconate dehydrogenase, encoded by the *gnd* gene, occurs at the posttranscriptional level and is mediated by a negative control element that lies deep in the coding sequence, somewhere between codons 48 and 118. Deletion analysis of a growth-rate-regulated *gnd–lacZ* translational fusion showed that the element is the segment of gnd mRNA between codons 67 and 78 that is complementary to an extensive portion of the *gnd* ribosome-binding site, including its Shine–Dalgarno sequence. The boundaries of the element were further defined by the cloning of a synthetic "internal complementary sequence." The core internal complementary sequence element effected growth-rate-dependent regulation when placed at several sites between codon 40 and codon 69, but it severely reduced gene expression when moved to codon 13. The effect on regulation of single and double mutations introduced into the element by site-directed mutagenesis correlated with the ability of the respective mRNAs to fold into secondary structures that sequester the ribosome-binding site. Thus the *gnd* gene's internal regulatory element appears to function as a cis-acting antisense RNA.**

Bacterial cells coordinate the rates of synthesis of rRNA, tRNA, and proteins with the cellular growth rate by a process called growth-rate-dependent regulation. Most studies of the mechanisms underlying this fundamental genetic regulatory process have been of ribosomal genes (reviewed in ref. 1). As a model system for growth-rate-dependent regulation of non-ribosomal genes, we have been studying the *Escherichia coli* K-12 *gnd* gene, which codes for the hexose monophosphate shunt enzyme, 6-phosphogluconate dehydrogenase (6PGD; EC 1.1.1.44) (reviewed in ref. 2). The mechanism responsible for this growth-rate-dependent regulation is unusual. It operates at the posttranscriptional level (3) and depends on a site that lies deep within the 6PGD coding sequence (4).

The existence of the *gnd* gene's internal regulatory region was revealed by the properties of a set of eight strains carrying *gnd–lacZ* protein (translational) fusions at the *gnd* locus of the chromosome (4). In these strains, the *gnd* promoter, *gnd* ribosome-binding site (RBS), and increasing amounts of the *gnd* structural gene are fused in-frame to codon 8 of *lacZ*. With seven of the fusion strains, which have 118 or more N-terminal codons of *gnd* fused to *lacZ*, expression of β-galactosidase is as growth rate dependent as that of 6PGD from a normal *gnd* gene. Thus all sites for the growth-rate-dependent regulation lie upstream from codon 118. The remaining fusion, which has only 48 N-terminal *gnd* codons, confers a growth-rate-derepressed phenotype, in that at low growth rates the level of β-galactosidase is 3 times higher than the level in the other fusion strains under the same growth conditions. Thus the region between codons 48 and 118 contains a negative control site involved in the growth-rate-dependent regulation of 6PGD level (4).

In this report, we use deletion analysis of a growth-rate-regulated *gnd–lacZ* translational fusion to delimit more precisely the 3′ boundary of the internal negative control element. The regulatory element lies within the "internal complementary sequence" (ICS, formerly called IHS), the 38-nucleotide segment of gnd mRNA spanning codons 67–78, which is highly complementary to the Shine–Dalgarno sequence (SD) and surrounding nucleotides of the *gnd* RBS. The ICS and its capacity to sequester the RBS in an mRNA secondary structure are conserved in the *gnd* genes of *Salmonella typhimurium* and *E. coli* strains isolated from natural populations (5, 6). By synthesizing an oligonucleotide containing the central 16 nucleotides of the ICS and placing it at several sites closer to the beginning of the gene, we show that a core element containing the anti-SD can mediate growth-rate-dependent regulation. A single base change within the anti-SD of the element causes growth-rate-derepressed expression of a *gnd–lacZ* translational fusion. Thus, the negative control element appears to function as a cis-acting antisense RNA even though it is located more than 200 nucleotides from its site of action. A model for growth-rate-dependent regulation of *gnd* expression is described.

MATERIALS AND METHODS

Bacterial Strains and Bacteriophage. Growth rate dependence of β-galactosidase expression from the various *gnd–lacZ* fusions was determined in monolysogens of strain HB301 [Δ(*argF–lac*)169], which is a derivative of the standard *E. coli* K-12 strain W3110. Phage λ RZ5 (obtained from R. Zagursky, E. I. DuPont de Nemours) was used for the transfer by *in vivo* recombination of *gnd–lacZ* fusions from plasmids to λ. The *b* region of λ RZ5 contains the C-terminal coding sequence of the pBR322 *bla* gene and a *lac* operon segment that includes the C-terminal coding sequence of *lacZ*, all of *lacY*, and the N-terminal coding portion of *lacA*.

Recombinant DNA Techniques. BAL-31 deletion mutagenesis was done by the method described by Silhavy *et al.* (7). Other recombinant DNA techniques were done as described by Maniatis *et al.* (8). DNA sequencing used plasmid templates (9).

Plasmids and Construction of 3′ Deletions. The starting plasmid for the preparation of 3′ deletions, pCM7 (Fig. 1), was derived from pHB580 (4) by deleting an IS5 element that lies upstream of the *gnd* promoter (5). The deletion extended to −135 with respect to the start of *gnd* transcription. In

The publication costs of this article were defrayed in part by page charge payment. This article must therefore be hereby marked "*advertisement*" in accordance with 18 U.S.C. §1734 solely to indicate this fact.

Abbreviations: 6PGD, 6-phosphogluconate dehydrogenase; SD, Shine–Dalgarno sequence; RBS, ribosome-binding site; ICS, internal complementary sequence.

*To whom reprint requests should be addressed.

control experiments growth-rate-dependent expression in strains monolysogenic for phage prepared from pCM7 was the same as for phage prepared from pHB580.

To prepare the 3′ deletions, pCM7 was digested with *Kpn* I, which cleaves uniquely at codon 124 of the *gnd* structural gene, and then treated for different lengths of time with BAL-31 exonuclease. The ends were made flush, *Bam*HI linkers were added, and the DNA was digested with *Bam*HI, which removed the remaining DNA between codon 124 and codon 8 of *lacZ*. The molecules were isolated from an agarose gel after electrophoresis (10) and self-ligated. Ampicillin-resistant, Lac$^+$ transformants of strain MC1000 [Δ(*lac*)] were selected, and the specific deletion endpoints were identified by DNA sequencing. All of the plasmids chosen for subsequent study had in-frame fusions of *gnd* to *lacZ* and a single *Bam*HI linker at the fusion joint. The control plasmid with 48 N-terminal *gnd* codons fused to *lacZ*, pHB543, has been described (4).

Lysogens. The *lac* and *bla* sequences present in both λ RZ5 and the *gnd–lacZ* fusion plasmids allow for the transfer, by *in vivo* genetic recombination, of fusions from plasmids to λ. The crosses were done by infecting cultures of strains carrying *gnd–lacZ* fusion plasmids with a single plaque of λ RZ5 as described (7). Strain HB301 was infected with the resulting lysates, and the mixture was spread on lactose MacConkey agar medium. The frequency of red, Lac$^+$ plaques was 10^{-3}–10^{-4}. Turbid, uniformly red plaques contained the desired recombinant phages, which were purified by single plaque isolation. Cultures of strain HB301 were infected with the recombinant phage, and Lac$^+$ lysogens were selected by streaking on lactose MacConkey agar containing ampicillin at 10 μg/ml. Lysogens were purified by several rounds of single colony isolation on indicator medium without ampicillin. Monolysogens were identified by a plaque test with phage λ *c*I *c*17 (11). The presence of the prophage at *att*λ was verified by transduction with a phage P1 lysate prepared on a *galE*::Tn*10* strain.

Synthesis and Cloning of the Core ICS. A mixture of single-stranded oligonucleotides with 2-fold degeneracies at two positions in the ICS was prepared with an automated DNA synthesizer. The mixture was cloned between the *Kpn* I and *Bam*HI sites of pCM7 as described in detail elsewhere (12). Aside from having nucleotides at each end that are complementary to the protruding bases generated by cleavage of DNA with *Kpn* I and *Bam*HI, the 30-mers contained the 16-nucleotide sequence of the DNA strand coding for the core of the ICS (or mutations of it) and a *Bgl* II recognition site, to facilitate subsequent recloning. The orientation and sequence of a 30-mer cloned into pCM7 is underlined in the sequence shown below:

```
5'-----GGTAC                                  GATCC-----3'
  gnd                                                lacZ
3'-----CCATGTCTAGAGTAGGACAATTACCACCTAGG-----5'
                    C T
```

Plasmids containing the wild-type ICS, the two single ICS mutations, and the double mutation were identified by DNA sequencing.

Placement of the Core ICS at Different Sites in *gnd*. The four ICS-containing plasmids were digested with *Bgl* II, which cleaved within the cloned 30-mer, and with *Pst* I, which cleaved uniquely in *bla*. Fragments containing the ICS, *lacZ*, and the C-terminal coding sequence of *bla* were purified by agarose gel electrophoresis. The plasmids with the 3′ deletions were digested with *Bam*HI and *Pst* I, and the fragments containing the N-terminal coding sequence of *bla*, the *gnd* promoter, and *gnd* N-terminal codons were purified by electrophoresis. The desired combinations of fragments were ligated together, and the reconstructed fusion plasmids were recovered by selection of ampicillin-resistant, Lac$^+$ transformants. The DNA sequence of the ICS and the *gnd–lacZ* fusion joint was determined for each plasmid.

Growth Conditions and Enzyme Assays. Physiological experiments were carried out as described (13) by using minimal medium with acetate or glucose as the carbon source. The growth rate constants [k = ln 2/mass doubling time (in hours)] were 0.16 ± 0.02 (mean ± standard deviation) for growth on acetate and 0.58 ± 0.03 for growth on glucose. β-Galactosidase activity was assayed in cells permeabilized by treatment with chloroform and SDS and expressed in Miller units (14).

RESULTS

Deletions Defining the 3′ Boundary of the Internal Negative Control Element. In-frame *gnd–lacZ* translational fusions with fusion joints in the codon 48–codon 118 segment of *gnd* were isolated and characterized. The starting plasmid for the deletion analysis, pCM7 (Fig. 1), carried the growth-rate-regulated fusion from pHB580 (4); its *gnd* DNA extends from −135 with respect to the start of transcription to codon 217 in the structural gene. The new fusions were prepared by making deletions that extend from the *Kpn* I site at codon 124 toward the start codon and lack the DNA between the *Bam*HI site at the fusion joint and the *Kpn* I site. Deletion endpoints were determined by DNA sequencing of small-scale plasmid preparations. Plasmids with 13, 40, 53, 64, 69, 71, 78, 87, 90, 111, and 124 N-terminal *gnd* codons fused in-frame to codon 8 of *lacZ* by means of a *Bam*HI linker were chosen for further study. To analyze growth-rate-dependent expression, the fusions were transferred by genetic recombination from the respective plasmids to λ RZ5, and strains monolysogenic for each of the resulting λ *gnd–lacZ* fusion phage were prepared. As controls, monolysogens were also prepared in the same manner from pCM7 and from a derivative of plasmid pHB543, which has 48 N-terminal *gnd* codons fused to *lacZ* and which confers growth-rate-derepressed expression (4).

The level of β-galactosidase was determined in cultures of the monolysogens growing exponentially in acetate and glucose minimal media (Fig. 2). As observed previously (4), the fusions fall into two classes of growth-rate-dependent expression. Expression of fusions with 78 or more N-terminal *gnd* codons, including the HB580 control fusion with 217 N-terminal *gnd* codons, was repressed during growth on acetate and induced about 1.4-fold by growth on glucose. In contrast, expression of fusions with 71 or fewer N-terminal *gnd* codons, including the HB543 control fusion with 48 N-terminal *gnd* codons, was growth rate derepressed in that the level of β-galactosidase in acetate-grown cultures was about 3-fold higher than in the acetate cultures of the other fusions; moreover, expression from this second group of fusions did not increase with increasing growth rate and, in fact, the level was slightly reduced by growth on glucose.

The clear-cut separation on the *gnd* map between the two classes of fusions shows that the 3′ boundary of the internal negative control element is between codons 71 and 78 of the *gnd* structural gene. This boundary lies within the segment of gnd mRNA, the ICS, that is highly complementary to the RBS, including its SD (2, 6). A computer-modeling algorithm for RNA secondary structure (15) suggested that the most thermodynamically stable structure of a gnd mRNA molecule containing the leader and 78 N-terminal codons has the RBS–ICS stem–loop domain (Fig. 3). Formation *in vivo* of such an intramolecular base-paired structure would be expected to block ribosome binding and thus reduce the frequency of translation initiation. If the ICS were to function as a cis-acting antisense RNA, it would fulfill the regulatory requirements defined by the properties of the transcriptional and translational fusions for a negative control element that acts at the posttranscriptional level.

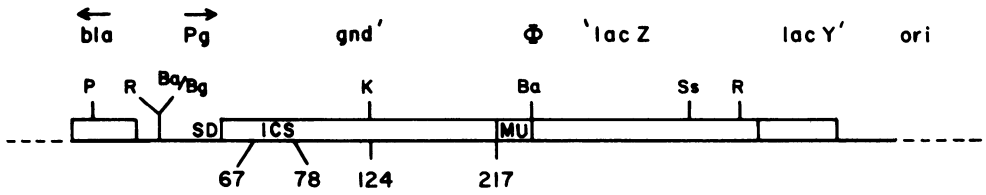

FIG. 1. Restriction map of plasmid pCM7. The numbers below the line are codons in the *gnd* structural gene. Restriction cleavage sites shown are R, *Eco*RI; Ba/Bg, hybrid *Bam*HI–*Bgl* II site; K, *Kpn* I; Ss, *Sst* I. P_g, *gnd* promoter; Mu, Mu*s* DNA from the original HB580 fusion; Φ, fusion joint between *gnd*, Mu, and *lac* DNA.

The growth rate induction ratios for the two types of fusions described here are different from the values obtained previously for growth-rate-inducible and growth-rate-derepressed fusions. In the previous study, fusion HB580 produced 2100 and 700 units of β-galactosidase during growth on glucose and acetate, respectively, for an induction ratio of 3.0 (4), whereas in the present study the fusion produced 930 and 530 units of activity during growth on the two carbon sources, an induction ratio of 1.8. Similarly, fusion HB543 produced 2400 and 1800 units of β-galactosidase during growth on glucose and acetate, respectively, in the earlier study (4) and 1800 and 2300 units of activity during growth on the two carbon sources in the present study. The constructions used in the two studies differ with respect to the chromosomal location of the fusions, *attλ* in the present study and the normal *gnd* region of the chromosome in the earlier experiments. The differences in expression are due to the differences in chromosomal location of the fusions because, when the λ phages carrying the control fusions were integrated at *gnd* in a Δ*attλ* Δ*lac* strain, the growth-rate-dependent expression characteristic of the original fusions was restored (V. Srinivas, H. Jiang, P.C.-M., and R.E.W., Jr., unpublished data). Presumably, chromosome position affects transcription initiation from the *gnd* promoter in a growth-rate-dependent manner. In any event, the two classes of fusions characterized in this work (namely, those with 78 or more *gnd* codons and those with 71 or fewer *gnd* codons) are the same as the original growth-rate-inducible and growth-rate-derepressed fusions represented by strains HB580 and HB543.

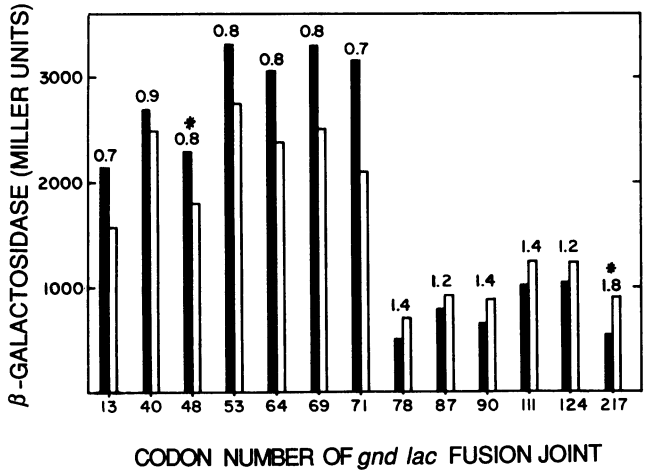

FIG. 2. Growth rate dependence of β-galactosidase level in strains monolysogenic at *attλ* for phages carrying *gnd–lacZ* translational fusions. Strains were grown in glucose (open bars) and acetate (filled bars) minimal media and assayed for β-galactosidase activity. The height of the bars indicates the amount of β-galactosidase, and the abscissa shows the number of N-terminal *gnd* codons fused to *lacZ* in each lysogen. The numbers above the columns are the ratios of the activities in the cultures grown on glucose to the activities in the acetate-grown cultures (i.e., the growth rate induction ratios). Bars marked with an asterisk indicate control monolysogens, which carry the HB543 (codon 48) and HB580 (codon 217) fusions (4) at *attλ*.

The Core ICS Mediates Growth-Rate-Dependent Regulation from Different Sites in *gnd*. We next wanted to examine the possibility that other sites essential for growth-rate-dependent regulation lie in the 6PGD coding sequence between the start codon and the ICS. We also wanted to determine whether the entire codon 67–codon 78 ICS element is necessary for the regulation. Rather than addressing these questions by isolating and characterizing other sets of deletions (e.g., 5′ deletions extending from the start codon toward the ICS), we synthesized a deoxyoligonucleotide containing the codon 69–codon 74 core of the ICS, cloned it by a newly designed method (12), and then constructed a new set of *gnd–lacZ* translational fusions in which the core ICS was placed at the junction between each of the 3′ deletion endpoints described above and codon 8 of *lacZ* (see *Materials and Methods*). The fusions were transferred to λ RZ5, and the growth rate dependence of β-galactosidase was determined in strains monolysogenic for each of the fusion phages.

Table 1 shows that the core ICS is able to mediate repression of β-galactosidase expression in cells growing on acetate from any location in *gnd* between codon 13 and its normal position. In the fusion strains in which the ICS is preceded by 40, 53, 64, or 69 N-terminal *gnd* codons, the level of expression in acetate-grown cells is similar to that of the control strain, whose fusion has 78 *gnd* codons (i.e., when the ICS is at its normal position in *gnd*). Moreover, in these strains the growth rate induction mediated by the core ICS is similar to that of the control fusion, which has the entire ICS. These data suggest that the core ICS can mediate both aspects of growth-rate-dependent regulation, repression un-

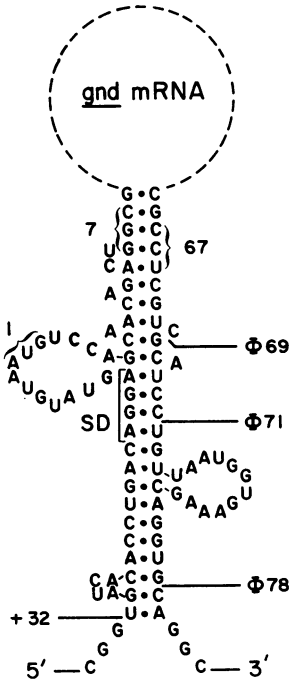

FIG. 3. Secondary structure of gnd mRNA involving complementary pairing between the RBS and the ICS. The RBS-containing segment of the intramolecular structure extends from approximately the middle of the gnd mRNA leader [+32 with respect to the transcription start point (16)] to codon 8 of the *gnd* structural gene; the ICS-containing segment extends from codon 66 to codon 78. The SD is in brackets and the start codon in parentheses. The structure was generated by a microcomputer and the RNA folding program of Zucker and Stiegler (15) for the gnd mRNA molecule through codon 78. Fusions at codons 69 and 71 confer growth-rate-derepressed phenotypes while the fusion at codon 78 is growth rate inducible (see Fig. 2).

Table 1. Regulation by ICS located various distances from the RBS

Fusion*	ICS†	Enzyme activity‡ Acetate	Glucose	Ratio§
Control	Wild type	499	686	1.4
69	−	3271	2496	0.8
69	+	761	944	1.2
64	−	3043	2377	0.8
64	+	441	498	1.1
53	−	3274	2756	0.8
53	+	270	528	1.9
40	−	2678	2480	0.9
40	+	758	909	1.2
13	−	2134	1579	0.7
13	+	41	11	0.3

*The control is the fusion from Fig. 2 that has 78 N-terminal *gnd* codons and the entire ICS located at its normal position in the gene. The numbers designate the number of N-terminal *gnd* codons fused in-frame to *lacZ*. The fusions are carried on single λ prophages located at *attλ*. The data for the fusions without the ICS are those of Fig. 2.

†+ and − indicate the presence or absence, respectively, of the synthetic core ICS at the fusion joint between *gnd* and *lacZ*.

‡β-Galactosidase activity was assayed in cells grown in acetate and glucose minimal media.

§The ratio of the enzyme level in glucose-grown cells to the level in acetate-grown cells.

der slow growth conditions and growth rate induction, and that there are no sites essential for the regulation in the codon 40–codon 69 segment of *gnd*.

The phenotype conferred by the fusion with the ICS at codon 13 was more complex. When located at codon 13, the ICS repressed expression about 50-fold during growth on acetate and about 150-fold during growth on glucose, much more severely than when located at the other sites. The simplest explanation for this drastically reduced expression is that placing the ICS close to the beginning of the gene significantly increases its ability to compete with ribosomes for the RBS and hence increases the fraction of mRNA molecules in the RBS–ICS inhibitory structure. In addition, the RBS–ICS stem–loop structure should be more stable than the structures formed when the ICS is located further away because the loop is smaller.

Mutations in the Anti-SD Portion of the ICS. To test directly the importance of the anti-SD segment of the ICS in growth-rate-dependent regulation, we introduced mutations into it. The synthetic core ICS described above was actually obtained from an oligonucleotide mixture that contained the wild-type sequence, a cytosine to guanine mutation at the second position of the TCCT anti-SD, a thymine to adenine mutation at the fourth position, and the corresponding double mutation. The oligonucleotide mixture was cloned, and the four different sequences were identified by DNA sequencing. The single and double mutations of the core ICS were placed at the fusion joints of the codon 40 and codon 69 fusions, and the growth rate dependence of the β-galactosidase level was assayed in monolysogens carrying the respective λ *gnd–lac* fusion phages integrated in single copy at *attλ*.

Fig. 4 shows the effects of the mutations on growth-rate-dependent expression of the *gnd–lacZ* fusions with 40 and 69 N-terminal *gnd* codons. For cells grown on acetate, the level of β-galactosidase in the fusions with the thymine to adenine mutation was about 3-fold higher than the level in the corresponding strain with the wild-type core ICS; for cells grown on glucose, the level in the thymine to adenine mutants was elevated about 2-fold. Thus a single base change in the anti-SD is sufficient to confer a growth-rate-derepressed phenotype. This result supports the hypothesis that the ICS mediates regulation by sequestering the RBS into a hairpin

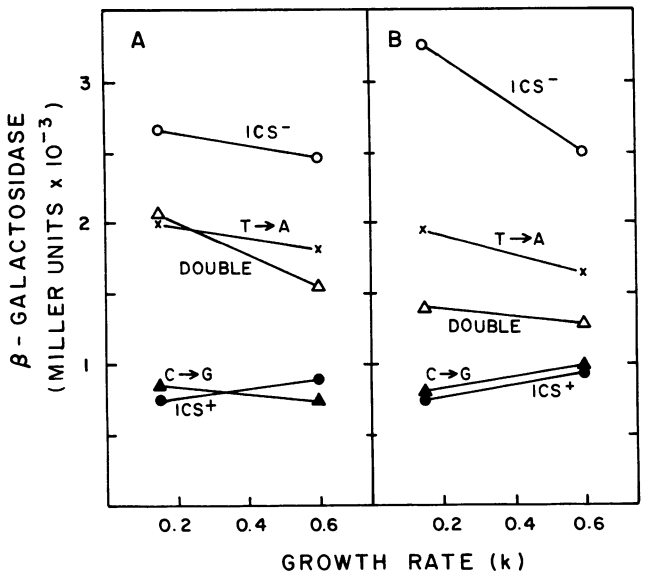

FIG. 4. Effect of mutations in the anti-SD on growth-rate-dependent expression of *gnd–lacZ* fusions in monolysogens. Fusions lacking the ICS (i.e., the 3′ deletions) or containing the wild-type core element or the element with thymine to adenine, cytosine to guanine, or double mutations in the anti-SD were prepared on plasmids and transferred to λ RZ5. Monolysogens of each phage were grown in acetate and glucose minimal media and assayed for β-galactosidase activity. (*A*) Fusions with 40 N-terminal *gnd* codons. (*B*) Fusions with 69 N-terminal *gnd* codons.

structure. Changing the second position of the anti-SD from a cytosine to guanine, however, had virtually no effect on growth-rate-dependent expression, and expression from the double mutants was partially derepressed, as if the thymine to adenine mutation is partially epistatic to the cytosine to guanine mutation.

The Zucker–Stiegler algorithm (15) was applied to the codon 40 and codon 69 sets of mutant mRNAs, which included 20 codons of *lacZ*. The most stable structures of both sets of mRNAs correlated perfectly with the phenotypes conferred by the various mutations (data not shown). According to the algorithm, which employed the RNA folding rules of Tinoco *et al.* (17), the RBS–ICS hairpin is not formed by the mRNAs with the thymine to adenine mutation, whereas an RBS–ICS hairpin slightly different from the wild-type structure but of similar stability is formed by the mRNAs with the cytosine to guanine mutation. The mRNAs with both mutations form an RBS–ICS hairpin as part of the most stable mRNA structure, but the hairpin is shorter and sequesters fewer of the bases of the RBS.

DISCUSSION

Using *gnd–lacZ* translational fusions, we show here that a 16-nucleotide sequence located at codons 69–74 of the *gnd* structural gene is a negative control element that is able to mediate both aspects of growth-rate-dependent regulation of *gnd* expression, repression under slow growth conditions, and induction during faster growth. Expression of fusions lacking the regulatory element is high under both slow and fast growth conditions, whereas expression of fusions containing the element is repressed during growth on acetate and, provided the distance between the element and the start codon is not less than 40 codons, induced by growth on glucose. The negative control element contains an anti-SD and overall is highly complementary to the *gnd* RBS. The correlation between the ability of wild-type and mutant fusion mRNAs to form a ribosome-occluding secondary structure and the phenotypes conferred by the respective fusions

strongly suggests that the element functions as a cis-acting antisense RNA. This conclusion is consistent with previous data that suggested that growth-rate-dependent regulation occurs at a posttranscriptional step in *gnd* expression (3). The element probably acts only in cis because growth-rate-dependent regulation of 6PGD level from an intact chromosomal *gnd* gene is unaffected by the presence of a high copy number plasmid carrying the promoter-proximal two-thirds of the gene, which includes the ICS (18). Moreover, a gnd^+ gene in trans has no effect on the growth-rate-derepressed expression of a protein fusion that lacks the ICS (4).

In formulating a model for growth-rate-dependent regulation of *gnd* expression that is based on the ICS functioning as a cis-acting antisense RNA, two questions must be addressed. (*i*) Given that transcription and translation are coupled in prokaryotes (19) (i.e., that ribosomes should be able to initiate translation at the *gnd* RBS before the ICS is synthesized), how can the inhibitory RBS–ICS structure ever form? (*ii*) How are changes in growth rate transmitted to *gnd*; i.e., what is the effector of the regulation, how does its action vary with growth rate, and how does it interact with the ICS?

A possible answer to the first question is that transcription of *gnd* may actually be uncoupled enough from translation to allow the RBS–ICS structure to form at the appropriate frequency. In fact, uncoupling could be the key control point for the growth-rate-dependent regulation. First, expression of an average gene is partially uncoupled during growth on acetate because the overall rate of mRNA transcription is greater than the corresponding rate of translation (20). Moreover, the degree of this natural uncoupling decreases with increasing growth rate such that coupling is complete during growth on glucose and at faster growth rates. This is because the rate of polypeptide chain elongation increases with increasing growth rate while the rate of mRNA transcription is constant (20).

Another way in which *gnd* expression might become uncoupled is based on the fact that the 5′ portion of the gnd mRNA leader contains sequences that are capable of sequestering the RBS into a secondary structure of moderate thermodynamic stability (6, 16). Initial formation of a leader–RBS structure would block translation initiation, uncouple transcription from translation, and ultimately allow the more stable RBS–ICS structure to form. Moreover, because ribosomes should compete with the 5′ leader sequence for the RBS, the concentration of ribosomes able to initiate translation could be the growth-rate-dependent parameter that effects the growth rate control of *gnd* expression. Thus, by this argument, as the concentration of free ribosomes increases with increasing growth rate (20, 21), the degree of uncoupling and hence the frequency of formation of the inhibitory RBS–ICS structure would decrease.

An endoribonuclease that recognizes the RBS–ICS structure could also be the effector of growth rate control of *gnd* expression. Nilsson *et al.* (22) have shown that the growth-rate-dependent synthesis of chloramphenicol acetyltransferase (CAT), encoded by the CAT gene of Tn*9*, and the major outer membrane protein OmpA can be accounted for by a growth-rate-dependent increase in the stability of the respective mRNAs. More recently, the stability of ompA mRNA was correlated with specific endonucleolytic cleavages in the 5′ noncoding region of the mRNA (23).

Accessibility of the SD and/or start codon to ribosomes is now well established as a key factor in determining the yield of polypeptide per mRNA. Mutations that increase the thermodynamic stability of ribosome-occluding intramolecular structures decrease translational efficiency and vice versa (24–27). Although much of the information about the effects of mRNA secondary structure on translational efficiency has been prompted by genetic engineering efforts aimed at maximizing gene expression (25, 27), intramolecular structures not only occur naturally in prokaryotes but several are known to be targets for genetic regulation (28, 29). In most ribosome-occluding secondary structures, the distance between the complementary sequences in the mRNA is small, usually less than 10 nucleotides. Thus, the *gnd* RBS–ICS structure is notable because the distance between the RBS and the ICS is over 200 nucleotides. The ability of two widely separated complementary sequences to form an RNA duplex that inhibits translation has precedence in trans-acting antisense RNAs (30–32).

We thank R. Zagursky for λ RZ5, M. Zucker for the RNA folding program, and D. Court for λ *c*I *c*17. This research was supported by Public Health Service Grant GM27113 from the National Institute of General Medical Sciences.

1. Jinks-Robertson, S. & Nomura, M. (1987) in *Escherichia coli and Salmonella typhimurium: Cellular and Molecular Biology*, eds. Neidhardt, F. C., Ingraham, J. L., Low, K. B., Magasanik, B. & Umbarger, H. E. (Am. Soc. Microbiol., Washington, DC), Vol. 2, pp. 1358–1385.
2. Wolf, R. E., Jr. (1985) in *Molecular Biology of Bacterial Growth*, eds. Schaecter, M., Neidhardt, F. C., Ingraham, J. L. & Kjeldgaard, N. O. (Jones & Bartlett, Boston), pp. 202–211.
3. Baker, H. V., II, & Wolf, R. E., Jr. (1983) *J. Bacteriol.* **153,** 771–781.
4. Baker, H. V., II, & Wolf, R. E., Jr. (1984) *Proc. Natl. Acad. Sci. USA* **81,** 7669–7673.
5. Barcak, G. J. & Wolf, R. E., Jr. (1988) *J. Bacteriol.* **170,** 365–371.
6. Barcak, G. J. & Wolf, R. E., Jr. (1988) *J. Bacteriol.* **170,** 372–379.
7. Silhavy, T., Berman, M. L. & Enquist, L. (1984) *Experiments with Gene Fusions* (Cold Spring Harbor Lab., Cold Spring Harbor, NY).
8. Maniatis, T. E., Fritsch, E. F. & Sambrook, J. (1982) *Molecular Cloning: A Laboratory Manual* (Cold Spring Harbor Lab., Cold Spring Harbor, NY).
9. Zagursky, R. J., Baumeister, K., Lomax, N. & Berman, M. L. (1985) *Gene Anal. Tech.* **2,** 89–94.
10. Struhl, K. (1985) *BioTechniques* **3,** 452–453.
11. Shimada, K., Weisberg, R. A. & Gottesman, M. E. (1972) *J. Mol. Biol.* **63,** 483–503.
12. Carter-Muenchau, P. & Wolf, R. E., Jr. (1987) *Gene Anal. Tech.* **4,** 105–110.
13. Wolf, R. E., Jr., Prather, D. M. & Shea, F. M. (1979) *J. Bacteriol.* **139,** 1093–1096.
14. Miller, J. H. (1972) *Experiments in Molecular Genetics* (Cold Spring Harbor Lab., Cold Spring Harbor, NY).
15. Zucker, M. & Stiegler, P. (1981) *Nucleic Acids Res.* **9,** 133–148.
16. Nasoff, M. S., Baker, H. V., II, & Wolf, R. E., Jr. (1984) *Gene* **27,** 253–264.
17. Tinoco, I., Jr., Borer, P. N., Dengler, B., Levine, M. D., Uhlenbeck, O. C., Crothers, D. M. & Gralla, J. (1973) *Nature (London) New Biol.* **246,** 40–41.
18. Farrish, E. E., Baker, H. V., II, & Wolf, R. E., Jr. (1982) *J. Bacteriol.* **152,** 584–594.
19. Miller, O. L., Jr., Beatty, B. R., Hamkalo, B. A. & Thomas, C. A. (1970) *Cold Spring Harbor Symp. Quant. Biol.* **35,** 505–512.
20. Bremer, H. & Dennis, P. P. (1987) in *Escherichia coli and Salmonella typhimurium: Cellular and Molecular Biology*, eds. Neidhardt, F. C., Ingraham, J. L., Low, K. B., Magasanik, B., Schaechter, M. & Umbarger, H. E. (Am. Soc. Microbiol., Washington, DC), Vol. 2, pp. 1527–1542.
21. Forchammer, J. & Lindahl, L. (1971) *J. Mol. Biol.* **55,** 563–568.
22. Nilsson, G., Belasco, J. G., Cohen, S. N. & von Gabain, A. (1984) *Nature (London)* **312,** 75–77.
23. Melefors, O. & von Gabain, A. (1988) *Cell* **52,** 893–901.
24. Hall, M. N., Gabay, J., Debarbouille, M. & Schwartz, M. (1982) *Nature (London)* **295,** 616–618.
25. Schoner, D. E., Hsiung, H. M., Belagaje, R. M., Mayne, N. G. & Schoner, R. G. (1984) *Proc. Natl. Acad. Sci. USA* **81,** 5403–5407.
26. McPheeters, D. S., Christensen, A., Young, E. T., Stormo, G. & Gold, L. (1986) *Nucleic Acids Res.* **14,** 5813–5826.
27. Lee, N., Zhang, S.-Q., Cozzitorto, J., Yang, J. S. & Testa, D. (1987) *Gene* **58,** 77–86.
28. Horinouchi, S. & Weisblum, B. (1981) *Proc. Natl. Acad. Sci. USA* **77,** 7079–7083.
29. Kastelein, R. A., Berkhout, B. & van Duin, J. (1983) *Nature (London)* **305,** 741–743.
30. Simons, R. & Kleckner, N. (1983) *Cell* **34,** 683–691.
31. Mizuno, T., Chou, M. Y. & Inouye, M. (1984) *Proc. Natl. Acad. Sci. USA* **81,** 1966–1970.
32. Krinke, L. & Wulff, D. L. (1987) *Genes Dev.* **1,** 1005–1013.